

# Dual role of an ac driving force and the underlying two distinct order-disorder transitions in the vortex phase diagram of $\text{Ca}_3\text{Ir}_4\text{Sn}_{13}$

Santosh Kumar,<sup>1,\*</sup> Ravi P. Singh,<sup>2,†</sup> A. Thamizhavel,<sup>2</sup> C. V. Tomy,<sup>1</sup> and A. K. Grover<sup>2,3</sup>

<sup>1</sup>*Department of Physics, Indian Institute of Technology Bombay, Mumbai 400076, India*

<sup>2</sup>*Department of Condensed Matter Physics and Materials Science,  
Tata Institute of Fundamental Research, Mumbai 400005, India.*

<sup>3</sup>*Department of Physics, Panjab University, Chandigarh 160014, India.*

## Abstract

We present distinct demarcation of the Bragg glass (BG) to multi-domain vortex glass (VG) transition line and the eventual amorphization of the VG phase in a weakly pinned single crystal of the superconducting compound  $\text{Ca}_3\text{Ir}_4\text{Sn}_{13}$  on the basis of comprehension of the different yields about the second magnetization peak (SMP) anomaly in the dc magnetization and the corresponding anomalous feature in the ac susceptibility measurements. The shaking by a small ac magnetic field, inevitably present in the ac susceptibility measurements, is seen to result in contrasting responses in two different portions of the field-temperature ( $H, T$ ) phase space of the multi-domain VG. In one of the portions, embracing the BG to VG transition across the onset of the SMP anomaly, the ac drive is surprisingly seen to assist the transformation of the well ordered BG phase to a lesser ordered VG phase. The BG phase exists as a superheated state over a small portion of the VG space and this attests to the first order nature of the BG to VG transition.

PACS numbers: 74.25.Ld, 74.25.Ha, 74.25.Op

Keywords: Peak effect, second magnetization peak, first-order transition

## I. INTRODUCTION

The advent of high  $T_c$  superconductivity [1] had made it enlightening and relevant to locate different phase boundaries in the  $H$ - $T$  phase space [2–9], depicting the various possible phase transformations for the vortex matter in a type-II superconductor. A widely investigated anomaly elucidating the features of the vortex phase diagram of a high  $T_c$  cuprate superconductor,  $\text{YBa}_2\text{Cu}_3\text{O}_7$  (YBCO) [9–16], has been the peak effect (PE) phenomenon [2], which amounts to a sudden increase in the otherwise monotonically decreasing critical current density ( $j_c$ ) just before reaching the upper critical field line,  $H_{c2}(T)$ . As per the Larkin-Ovchinnikov [17] description,  $j_c$  is related inversely to the volume ( $V_c$ ) ( $j_c \propto 1/\sqrt{V_c}$ ) of the domain within which the displacements of the individual flux lines remain well correlated. Hence, an anomalous increase in  $j_c(H, T)$  (as in PE phenomenon) signifies a shrinkage in  $V_c$ , which in turn, amounts to an order-disorder transformation of the vortex matter. Somewhat analogous to the PE, there is another anomalous feature occurring deep inside the mixed state (well below  $H_{c2}$ ), called the second magnetization peak (SMP) [9, 15, 16, 18–24] which also imprints as a non-monotonic behavior of  $j_c(H)$ . The SMP feature has been well studied in high  $T_c$  cuprate superconductors,  $\text{YBa}_2\text{Cu}_3\text{O}_7$  (YBCO) [9],  $\text{Bi}_2\text{Sr}_2\text{CaCu}_2\text{O}_8$  (BSCCO) [20, 21] and another oxide superconductor, (Ba,K)BiO system [22–24].

As an important consequence of the above mentioned

studies of the vortex phase transformations in the high  $T_c$  superconductors, the PE/SMP behavior and the vortex phase diagrams have been revisited various times in several conventional superconductors, such as, Nb [25–27],  $2\text{H-NbSe}_2$  [2, 3, 7, 28–33],  $\text{YNi}_2\text{B}_2\text{C}$  [34, 35],  $\text{LuNi}_2\text{B}_2\text{C}$  [34]  $\text{Ca}_3\text{Rh}_4\text{Sn}_{13}$  [16, 36–39],  $\text{Yb}_3\text{Rh}_4\text{Sn}_{13}$  [40, 41] etc.,. The order-disorder transitions (*a la* PE and SMP) reported in  $\text{Ca}_3\text{Rh}_4\text{Sn}_{13}$  (CaRhSn) by some of the present authors [16] bore a marked resemblance with characteristic results in some single crystals of the high  $T_c$  superconductor YBCO. In addition, a recent report [39] of an exemplification of the notion of inverse melting of the vortex lattice in a crystal of CaRhSn echoes well with the similar characteristic in the high  $T_c$  superconductors YBCO [42] and BSCCO [43]. The above mentioned investigations in the low  $T_c$  superconductors have thus lead to the revelation of many instructive aspects of the PE and the SMP anomalies. For example, the results of small angle neutron scattering (SANS) together with ac susceptibility measurements performed concurrently in a single crystal of Nb provided convincing evidence of a quasi-first-order transition, from flux line lattice to amorphous vortex solid, across the onset of the PE anomaly [26]. The SMP on the other hand, is widely accepted [9, 18, 19] as a disorder or pinning-induced transition amounting to a well ordered Bragg glass (BG) state transforming to a *multi-domain* vortex glass (VG) phase [4, 5, 20, 44]. The first-order nature of BG to VG transition, however, awaits convincing elucidation. In spite of advances in understanding and continuous updating of the vortex phase diagrams of a variety of type-II superconductors [32, 33, 35, 45], several issues still remained to be fully comprehended. One of these is the delineation between the SMP and PE anomalies when they juxtapose, and the underlying physics represented by them.

Motivated by the aforesaid interesting features re-

\*Electronic address: santoshkumar@phy.iitb.ac.in

†Department of Physics, Indian Institute of Science Education and Research, Bhopal 462066, India.

ported for a variety of superconductors, we have now investigated another low  $T_c$  ( $\sim 7.10$  K) [46–48] superconductor  $\text{Ca}_3\text{Ir}_4\text{Sn}_{13}$ , which belongs to the family of ternary stannides [49] having cubic structure. This compound has attracted particular attention in recent years. For example, there have been evidences for nodeless superconductivity [48] and a coexistence of superconductivity and ferromagnetic spin fluctuations [47] (attributed to Ir 4d-band) in  $\text{Ca}_3\text{Ir}_4\text{Sn}_{13}$ . However, to the best of our knowledge, studies related to vortex phase transformations in its superconducting mixed state have not been reported in this compound. In this work, we present a comparison of different outcomes of the ac and dc magnetization measurements performed in a weakly pinned (ratio of depinning and depairing current densities is  $\sim 10^{-5}$ ) single crystal of  $\text{Ca}_3\text{Ir}_4\text{Sn}_{13}$ . The magnetization data reveal a very broad composite anomalous variation in  $j_c(H, T)$  which amounts to an order-disorder transformation in the vortex matter, however, the specific phase boundaries, pertaining to the order-disorder transformation, obtained from the ac and the dc measurement techniques are found to be significantly different. We can identify a certain region of the phase space where the ac field unexpectedly assists the transformation of the quasi-ordered BG into the partially disordered VG phase. In a different region of the  $H$ - $T$  phase space, the ac drive is seen to enhance the quality of spatial order of the underlying vortex matter, which inter alia is indicative of another order-disorder transition occurring in that portion of phase space, which gets exposed under the influence of an ac field. The two contrasting roles of the ac drive in different portions are attributed to the juxtaposition of the SMP anomaly (pinning induced) and the peak effect (PE) phenomenon (collapse of elasticity induced amorphization of the vortex matter). The unusual outcome of the imposition of an ac drive near the onset field of SMP anomaly in the present report also corroborates a very recent finding [50] in a different class of superconductor, (i.e., in  $\text{Ba}_{0.5}\text{K}_{0.5}\text{Fe}_2\text{As}_2$ ), wherein a large ac field ( $\sim 12$  Oe) lowers the onset field value of the anomalous change in  $j_c$  at a given temperature, thereby elucidating the role of ac driving force in facilitating the spatial disordering of the vortex matter in a portion of the phase-space where the ordered state is metastable superheated state.

## II. EXPERIMENTAL DETAILS

The single crystals of  $\text{Ca}_3\text{Ir}_4\text{Sn}_{13}$  were grown by tin flux method [46]. The crystal chosen for the present study is platelet shaped, with a planar area of  $4.7\text{ mm}^2$  and with thickness of  $0.64\text{ mm}$ , and mass of  $26.2\text{ mg}$ . The ac and dc magnetization measurements were performed in a Superconducting Quantum Interference Device-Vibrating Sample Magnetometer (SQUID-VSM, Quantum Design Inc., USA). The amplitude of the vibration in SQUID-VSM was kept small for all the dc magnetization measurements so as to avoid artifact that could arise from

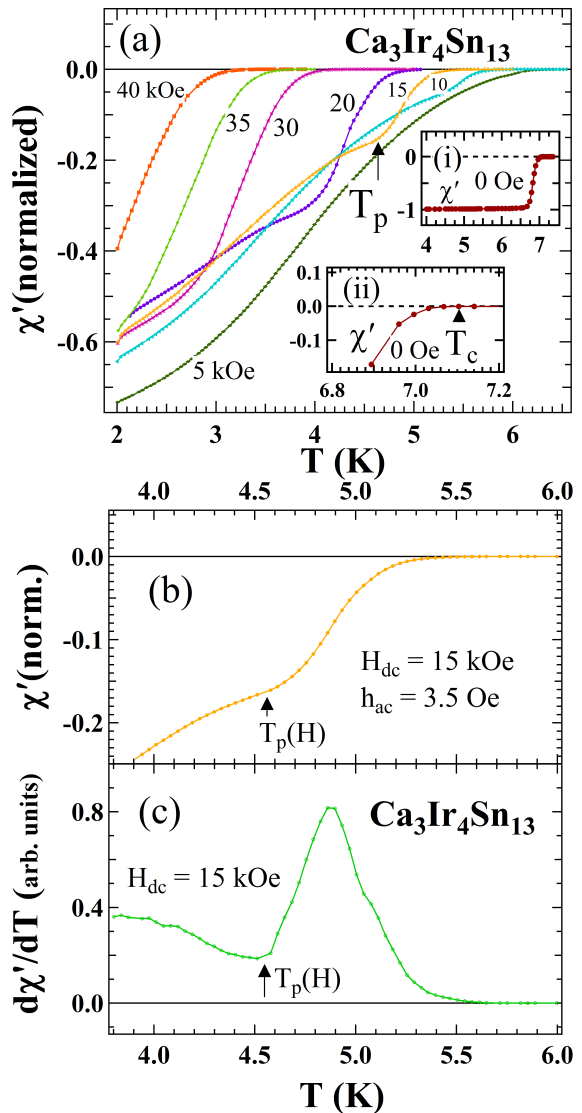


Figure 1: (Color online) (a) Real part of the ac susceptibility,  $\chi'(T)$  (in normalized units) plotted against temperature at various dc magnetic fields (applied parallel to the plane of platelet shaped crystal and as indicated). Inset (i) shows the saturated  $\chi'(T)$  response for  $H_{dc} = 0$ , and the inset (ii) displays its magnified portion near  $T_c$ . (b) Portion of  $\chi'(T)$  curve for  $H_{dc} = 15$  kOe showing an anomalous modulation prior to the transition to the normal state. (c) Portion of derivative plot of  $\chi'(T)$  (with respect to  $T$ ) for  $H_{dc} = 15$  kOe locating the temperature ( $T_p(H)$ ) corresponding to a position of a maximum in  $j_c(T)$ .

possible magnetic field inhomogeneity of a superconducting magnet along the length of sample movement. The ac magnetization measurements were performed by superimposing an oscillating magnetic field on various dc magnetic fields. The peak amplitude and the frequency of the driving ac field were chosen as  $3.5$  Oe and  $211$  Hz, respectively.

### III. RESULTS

#### A. Ac susceptibility: Identification of anomalous variation in critical current density.

##### 1. Isofield ac susceptibility measurements

Figure 1(a) shows the temperature dependences of the real part of the isofield ac susceptibility ( $\chi'(T)$ ) in dc fields (applied parallel to plane of the platelet shaped sample), as indicated. The  $\chi'(T)$  plots have been normalized with respect to the saturated value of  $\chi'$  recorded at  $T = 2$  K for  $H_{dc} = 0$ . The  $\chi'(T)$  curve for  $H_{dc} = 0$  shows the saturated behavior at low temperatures (see the inset (i) of Fig. 1(a)), revealing the characteristic full magnetic shielding effect, typical of a superconductor. The superconducting transition temperature,  $T_c(H_{dc} = 0) \approx 7.1$  K, obtained via the onset of diamagnetic response (see expanded plot in the inset (ii) of Fig. 1(a)) from this measurement agrees with the  $T_c$  reported for this compound in Ref. [47]. The  $\chi'(T)$  response for  $H_{dc} = 5$  kOe in the main panel of Fig. 1(a) shows a much broader transition to the normal state depicting the monotonically decreasing value of  $\chi'(T)$  as the temperature is increased. Since  $\chi'$  is related to the critical current density,  $j_c(H, T)$  ( $\chi' \sim -\beta j_c/h_{ac}$ ) [10], where  $h_{ac}$  is the amplitude of the ac drive and  $\beta$  depends on the size and geometry of the sample), the fall in  $|\chi'(T)|$  reflects a decrease in  $j_c(H, T)$  with increasing temperature. However, the  $\chi'(T)$  response for  $H_{dc} = 10$  kOe shows an unusual deviation from the smooth monotonic decrease prior to the superconducting to normal transition, which in turn indicates a possible non-monotonic behavior of  $j_c$ . This modulation in  $\chi'(T)$  becomes more pronounced for  $H_{dc} = 15$  kOe (marked by arrow) and for  $H_{dc} = 20$  kOe, but the same characteristic could not be identified clearly at higher fields ( $H_{dc} > 25$  kOe). In order to bring out the interesting characteristics of this modulation, we now examine in Fig. 1(b), the behavior of  $\chi'(T)$  near the region, where this modulation is observed for  $H_{dc} = 15$  kOe. This feature can be more clearly discerned in an expanded plot of the derivative of  $\chi'(T)$  with respect to  $T$  (see Fig. 1(c)). The point of inflection in  $\chi'(T)$ , where the slope is minimum, identifies the maximum in  $j_c$  as a function of temperature at a constant field. This temperature is marked as  $T_p(H)$  ( $\sim 4.56$  K). After  $T_p(H)$ , the slope  $d\chi'/dT$  increases abruptly, reaching a maximum value and then falling to a value close to zero.

##### 2. Isothermal ac susceptibility measurements

To further understand the details of the modulation in  $j_c(H, T)$  reflected in the isofield ac susceptibility measurements, we recorded isothermal ac susceptibility,  $\chi'(H)$ , data as well, where the above discussed anomalous trend could be observed more clearly over a wide range of temperatures ( $T \leq 5.5$  K), as shown in Fig. 2(a)

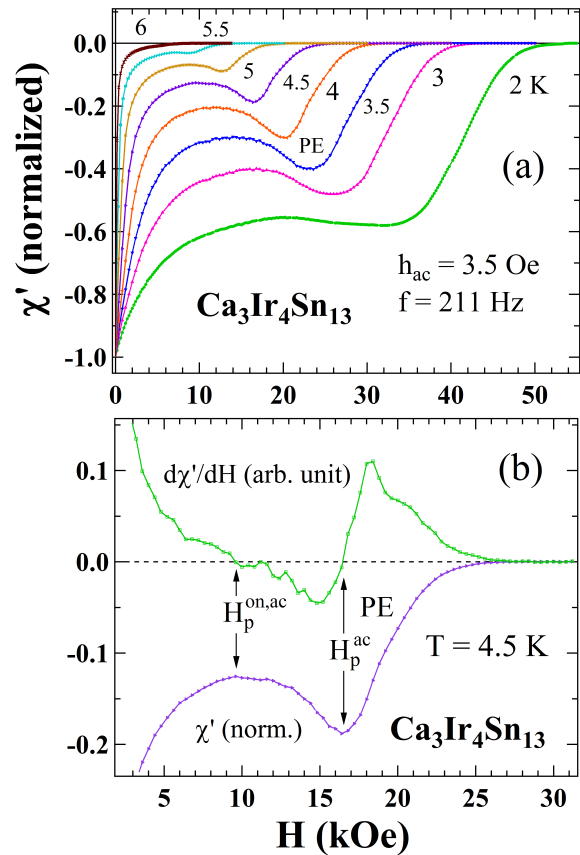


Figure 2: (Color online) (a) Isothermal ac susceptibility ( $\chi'(H)$ ) plotted against the dc magnetic field at various temperatures, as indicated. PE phenomenon could be observed for  $T < 5.5$  K. (b) Portions of  $\chi'(H)$  (in normalized units) and  $d\chi'/dH$  (in arbitrary units) plots at  $T = 4.5$  K. The first zero crossing in  $d\chi'/dH$  indicates the onset ( $H_p^{on,ac}$ ) of the PE, whereas the second one marks the peak field ( $H_p^{ac}$ ) of the PE.

( $\chi'(H)$  values are normalized with respect to their saturated value at  $H = 0$ ). The specimen was cooled in a nominal zero field down to a desired temperature and then the  $\chi'(H)$  data were recorded while increasing the dc field. The  $\chi'(H)$  response at each temperature initially decreases as the magnetic field is enhanced from zero field value, revealing the usual fall in  $j_c(H)$  with increasing field at a constant temperature. However, an anomalous dip in  $\chi'(H)$  response can be seen at higher field values. As the temperature is increased, the onset field values of this dip gradually shift towards lower field values (cf. Fig. 2(a)), reaching closer to the respective critical field values of superconducting-normal transition, which, in turn, suggests that the observed anomaly is akin to the well documented peak effect (PE) phenomenon [2, 3, 7–16, 25–38]. In Fig. 2(b), we show an expanded portion of  $\chi'(H)$  response at  $T = 4.5$  K, where the onset field ( $H_p^{on,ac}$ ) of the peak effect like feature and the peak field ( $H_p^{ac}$ ) of the PE are indicated by arrows. We further

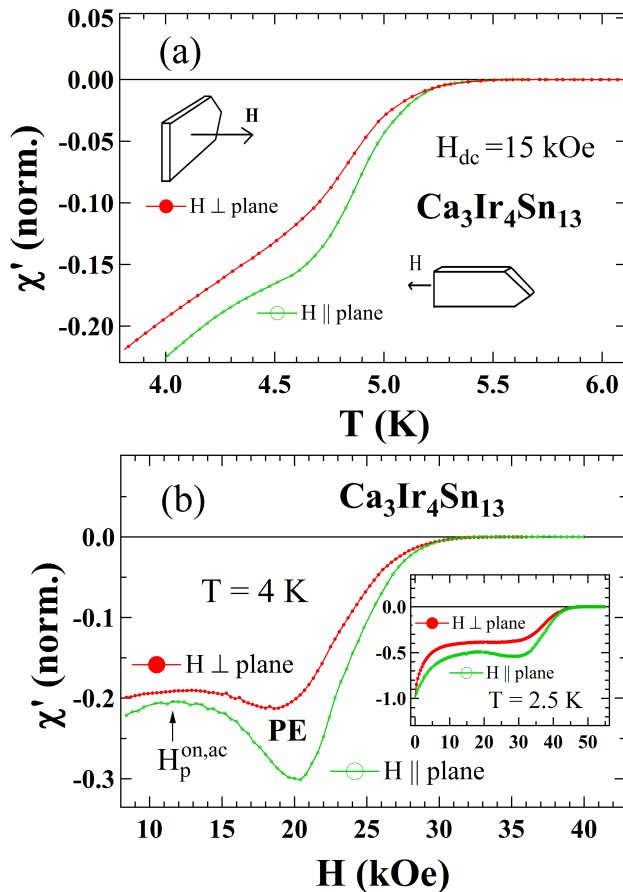


Figure 3: (Color online) (a) Temperature dependences of the ac susceptibility ( $\chi'(T)$ ) for dc field = 15 kOe, applied perpendicular as well as parallel to the plane of the platelet shaped crystal. The two orientations of the crystal (relative to field) are drawn in this panel. (b) Isothermal  $\chi'(H)$  response (normalized) for these two orientations of the crystal at  $T = 4$  K (main panel) and  $T = 2.5$  K (inset panel).

clarify the PE feature by plotting the derivative of  $\chi'$  with respect to  $H$  at  $T = 4.5$  K in the same panel. The derivative curve ( $d\chi'/dH$ ) in Fig. 2(b) may appear on first examination to be analogous to the derivative plot  $d\chi'/dT$  at  $H_{dc} = 15$  kOe (cf. Fig. 1(c)). However, it is to be noted that the derivative of  $\chi'(H)$  with respect to  $H$  in Fig. 2(b) has two zero crossings; the first one is taken to imprint the onset of peak effect like anomaly ( $H_p^{on,ac}$ ) and the second one identifies the peak position of the PE ( $H_p^{ac}$ ).

### 3. Sample geometry and anomalous variation in current density

The sample geometry and demagnetization factor can affect the state of the spatial order of vortex matter in a given sample due to edge effects [51, 52], which in turn could influence the triggering of the anomalous variation

in  $j_c$  in isofield/isothermal scans. This motivated us to measure the ac susceptibility with field applied normal to the plane of the  $\text{Ca}_3\text{Ir}_4\text{Sn}_{13}$  sample. We show in Fig. 3(a), a comparison of  $\chi'(T)$  in the two different orientations:  $H$  parallel and perpendicular to the plane of the sample. It is apparent that a deviation from the monotonically decreasing  $\chi'(T)$  is present across nearly identical temperature intervals in both the orientations. The anomaly is also present in isothermal  $\chi'(H)$  responses across similar field intervals for both the orientations; typical curves are shown for  $T = 4$  K (Fig. 3(b)) and  $T = 2.5$  K (an inset in Fig. 3(b)). Thus, we may conclude that the above stated features observed in the ac susceptibility are characteristic of the pinned vortex matter in the bulk of the  $\text{Ca}_3\text{Ir}_4\text{Sn}_{13}$  crystal. The anomalous peak feature is some-

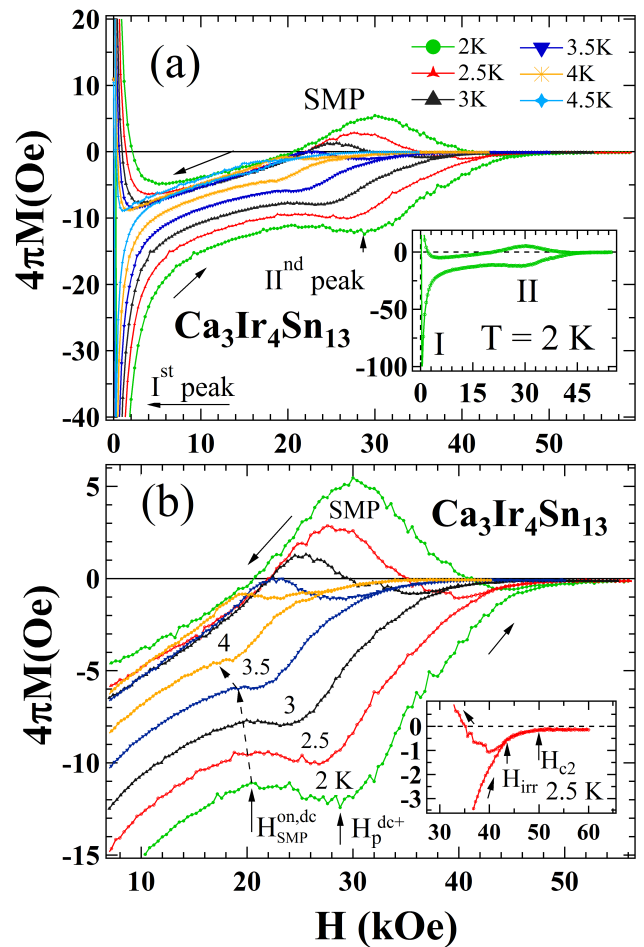


Figure 4: (Color online) (a) Isothermal  $M-H$  scans (first two quadrants) recorded at different temperatures, as indicated. Inset shows one typical  $M(H)$  curve recorded at  $T = 2$  K with the two peaks occurring in  $M(H)$  curve marked as I and II peak. (b) Expanded portions of the  $M(H)$  loops near an anomalous enhancement in hysteresis width ( $\Delta M = M(H \uparrow) - M(H \downarrow)$ ) obtained at different temperatures. The irreversibility field ( $H_{irr}$ ) and the upper critical field ( $H_{c2}$ ) have been located in the  $M(H)$  curve at  $T = 2.5$  K (see inset).

what less prominent for  $H$  perpendicular to the plane of the crystal, presumably due to the pinned vortex state being less spatially ordered prior to the PE in this orientation. The vortex phase boundaries determined from the characteristic features of the anomalous variation in  $j_c$  are however found to be not significantly dependent on the demagnetization factor and the sample geometry.

## B. Identification of the second magnetization peak (SMP): dc magnetization hysteresis loops.

### 1. Isothermal $M$ - $H$ scans

Figure 4(a) displays the first two quadrants of isothermal magnetization data, i.e.,  $M$ - $H$  loops recorded at various temperatures, for field applied parallel to the plane of the platelet sample. The sample was first cooled in nominal zero field down to a desired temperature and the magnetization was recorded while ramping the field @ 100 Oe/s well beyond the upper critical field, and then back to zero. Figure 4(b) presents the portions of  $M$ - $H$  loops in the vicinity of an anomalous enhancement seen in the hysteresis width ( $\Delta M(H) = M(H \uparrow) - M(H \downarrow)$ ). As per a prescription of the Bean's critical state model [53], the hysteresis width ( $\Delta M(H)$ ) of the  $M(H)$  curve is roughly proportional to  $j_c(H)$  [54]. Therefore, the second magnetization peak feature [9, 15, 16, 18-24] observed in the  $M(H)$  curves (Fig. 4) reflects an anomalous modulation in  $j_c(H)$ , which, in turn, could be indicative of an order-disorder transition in the vortex matter. The  $M(H)$  data show that the onset position (marked as  $H_{SMP}^{on,dc}$  in Fig. 4(b)) of this anomaly is nearly temperature-independent in the range  $2\text{ K} \leq T \leq 3.5\text{ K}$  (shown by a dashed arrow line in Fig. 4(b)). The onset field ( $H_{SMP}^{on,dc}$ ) of the characteristic anomalous feature is located far away from the threshold field value ( $H_{c2}$ ) of the superconducting-normal transition for  $T < 4\text{ K}$ , which is in contrast to the quintessential PE phenomenon typically located at the edge of the  $H_{c2}$  in very weakly pinned superconductors. The anomalous variation in  $j_c(H)$  located away from  $H_{c2}$  (see inset in Fig. 4(b) for location of  $H_{c2}$  at 2.5 K) is termed as the SMP anomaly. The inset in Fig. 4(b) also shows that the forward ( $M(H \uparrow)$ ) and reverse ( $M(H \downarrow)$ ) magnetization curves merge at a field identified as the irreversibility field,  $H_{irr}$ .

### 2. Magnetization response above the irreversibility field/temperature

Figure 5(a) illustrates a portion of the  $M$ - $H$  curve at  $T = 4.5\text{ K}$ , wherein one can note a large field interval of reversible magnetization beyond  $H_{irr}$ . It could be argued that the linear extrapolation of the nearly reversible magnetization beyond  $H_{irr}$  to the  $M = 0$  axis would lead to an estimate of the upper critical field  $H_{c2}$ , in accordance with the Ginzburg-Landau theory [55]. However,

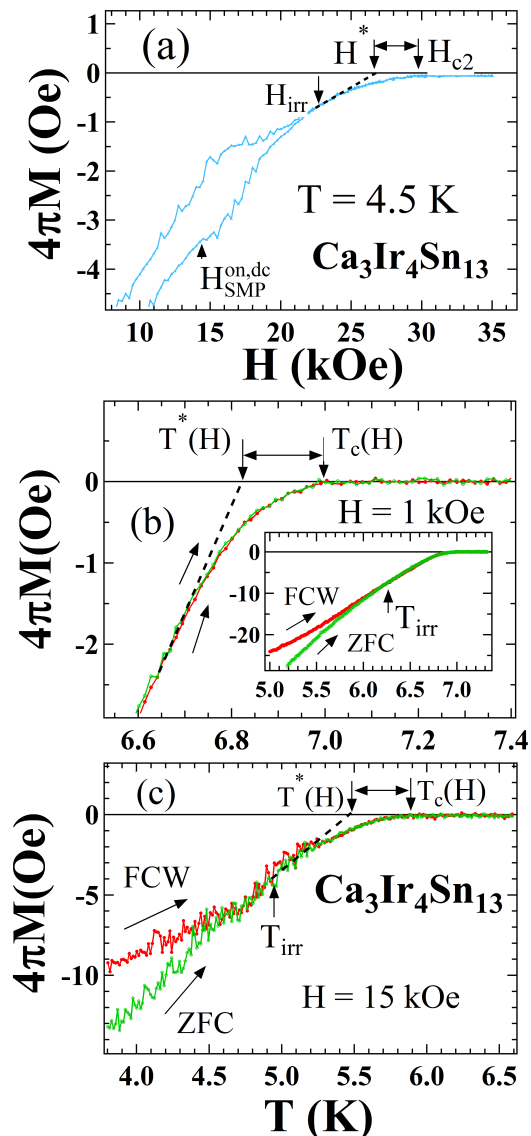


Figure 5: (Color online) (a) Portion of  $M$ - $H$  curve at  $T = 4.5\text{ K}$  near the superconducting-normal transition. The  $M$ - $H$  curve when linearly extrapolated (dotted lines) beyond  $H_{irr}$ , yields a characteristic field  $H^*$ . The onset of diamagnetism is marked as  $H_{c2}$  ( $> H^*$ ). Portions of ZFC and FCW curves obtained at  $H = 1\text{ kOe}$  (panel (b)) and  $H = 15\text{ kOe}$  (panel (c)). An inset in panel (b) shows the merger of ZFC and FCW occurring at  $T_{irr}$  for  $H = 1\text{ kOe}$ .

in the present case, the linear extrapolation of magnetization data beyond  $H_{irr}$  to the  $M = 0$  axis identifies another characteristic field,  $H^*(T)$ , which is significantly lower than the  $H_{c2}$  value marked in Fig. 5(a).

To further comprehend the behavior in  $M(H)$  response between  $H_{irr}$  and  $H_{c2}$ , we now draw attention to the isofield dc magnetization  $M(T)$  data plotted in Figs. 5(b) and 5(c). These two panels show the zero field-cooled (ZFC) and field-cooled warm-up (FCW) magnetization responses at  $H = 1\text{ kOe}$  (Fig. 5(b)) and  $H = 15\text{ kOe}$

(Fig. 5(c)). The sample was cooled in nominal zero field down to  $T \sim 2$  K, a field was applied and the magnetization was recorded while warming to obtain  $M_{ZFC}(T)$ . The sample was then cooled from  $T > T_c$  in the same field down to  $T \sim 2$  K and the magnetization was recorded while warming, which is the  $M_{FCW}(T)$ . It can be seen that the  $M_{ZFC}(T)$  and  $M_{FCW}(T)$  curves merge at a temperature, nominally marked as the irreversibility temperature  $T_{irr}$  (see the inset in Fig. 5(b), where this temperature is marked for  $H = 1$  kOe). Usually, a linear extrapolation of the (equilibrium) magnetization above  $T_{irr}$  to the  $M = 0$  axis is taken to identify the superconducting transition temperature  $T_c(H)$ . However, similar to the  $M(H)$  response near the superconducting transition (cf. Fig. 5(a)), there exists a nearly reversible diamagnetic response persisting up to a higher temperature, which we have marked as the critical temperature,  $T_c(H)$ . Thus, the linear extrapolation of  $M(T)$  curve above  $T_{irr}$  to the  $M = 0$  has been identified with a characteristic temperature  $T^*(H)$  ( $< T_c(H)$ ) in Figs. 5(b) and 5(c).

#### IV. DISCUSSION: THE VORTEX PHASE DIAGRAM

The results of both ac and dc magnetization measurements can finally be summarized by constructing a field-temperature ( $H$ - $T$ ) phase diagram for a given crystal of  $\text{Ca}_3\text{Ir}_4\text{Sn}_{13}$ . Figure 6 illustrates this phase diagram depicting the various vortex phases separated by the boundaries/crossover regimes, as indicated. The phase boundary corresponding to the onset of the peak anomaly in  $j_c(H)$  ( $H_p^{on,ac}$ ), as extracted from the ac  $\chi'(H)$  plots, lies significantly below than the onset of the SMP ( $H_{SMP}^{on,dc}$ ) line obtained from the dc  $M(H)$  curves. However, considering that both the SMP and the PE anomalies signify order-disorder transformation(s) in the vortex state, the region-I enclosed between the onset field values of the two anomalies, (viz. between  $H_p^{on,ac}(T)$  and  $H_{SMP}^{on,dc}(T)$  lines in the main panel of Fig. 6), is to be viewed as a well ordered vortex state via the dc  $M(H)$  measurements. The same field interval construes as a disordered region in view of the anomalous response observed in this region in the ac  $\chi'(H)$  measurements. The superposed ac magnetic field in the  $\chi'(H, T)$  measurements per se acts as an additional driving force on the pinned vortex matter. Such a driving force is typically known to transform a metastable vortex configuration towards an equilibrium configuration in a given  $(H, T)$  region [26, 56] by virtue of shaking the vortices around their mean locations. It is pertinent to recall here that from small angle neutron scattering measurements on the vortex matter in a weakly pinned crystal of Nb, Ling *et al.* [26], had vividly shown that metastable disordered/ordered states possible below/above the onset of the PE boundary transform to their equilibrium ordered/disordered states in the respective  $(H, T)$  regions on shaking with an ac drive. In this context, in the present situation in

$\text{Ca}_3\text{Ir}_4\text{Sn}_{13}$ , the observation of disordered configuration (region-I) in the ac  $\chi'(H)$  measurements below the onset position of the SMP line is counter-intuitive. It would be more appropriate to state that the ordered state is an equilibrium state only below  $H_p^{on,ac}(T)$  (shown by thick line in Fig. 6). The ordered configuration observable in dc magnetization measurements between  $H_p^{on,ac}(T)$  and  $H_{SMP}^{on,dc}(T)$  can thus be identified with the notion of superheating of the BG phase above the  $H_p^{on,ac}(T)$  line. The said superheated BG state transforms to its disordered version above the first order like  $H_p^{on,ac}(T)$  line under the influence of an ac driving force in region-I.

In Fig. 6, it is instructive to note further that  $H_p^{ac}(T)$  line lies above the  $H_p^{dc+}(T)$  line (the latter obtained from forward legs of the  $M(H)$  curves, cf. Fig. 4(b)). If the  $(H, T)$  region above  $H_p^{dc+}(T)$  line is to be viewed as an amorphous vortex matter, the  $H$ - $T$  phase space (i.e., region II) bounded between  $H_p^{dc+}(T)$  and  $H_p^{ac}(T)$  lines is such that an ac driving force is seen to improve the state of spatial order in the vortex matter in this region. This is in sharp contrast to the situation in region-I. On the basis of effect of an ac drive in this region (II), one can also argue that the peak field of the SMP ( $H_p^{dc+}$ ) marks the onset of another order-disorder transition; such an inference is possible only by combining the outcomes of the influence of an ac drive with those obtained from  $M(H)$  data, where such a drive is not present. The amorphised state of the vortex matter as an equilibrium state thus emerges above the  $H_p^{ac}(T)$  values (thick line in Fig. 6), instead of the usually presumed  $H_p^{dc+}(T)$  values (dotted line in Fig. 6), as marked from the dc  $M$ - $H$  scans. It may be added here that the  $H_p^{on,ac}(T)$  and  $H_p^{ac}(T)$  lines are independent of frequency in the range 10 Hz to  $10^3$  Hz in which we repeated the ac susceptibility measurements in our set up.

Considering that the onset ( $H_{SMP}^{on,dc}(T)$ ) of SMP is nearly temperature independent (for  $T < 4.5$  K) and is located far below the  $H_{c2}$  line in Fig. 6, we are lead to surmise that the  $H$ - $T$  region between  $H_{SMP}^{on,dc}$  and  $H_p^{dc+}$  as the multi-domain vortex glass (VG) state [4, 5, 20, 44], in comparison to the assigned nomenclature of Bragg glass (BG) to the vortex matter below the onset position of the anomalous variation in critical current density. In the absence of an ac drive, the BG extends up to  $H_{SMP}^{on,dc}(T)$  line, whereas in the presence of a drive, BG state would get restricted up to  $H_p^{on,ac}(T)$  line. We noted above that for  $T < 4.5$  K, the  $H$ - $T$  phase space between  $H_p^{on,ac}(T)$  and  $H_p^{ac}(T)$  lines can be subdivided notionally into three parts on the basis of effects of an ac drive on the underlying state of order in the vortex matter. Above  $T = 4.5$  K, we did not observe the fingerprint of SMP anomaly in the dc  $M$ - $H$  data. The  $(H$ - $T)$  region in dotted rectangular box in Fig. 6 pertains to  $(H$ - $T)$  phase space, where we observe only the PE anomaly in the ac  $\chi'$  data. In the boxed region,  $H_p^{on,ac}(T)$  line continues to mark the BG to multi-domain VG transition and  $H_p^{ac}(T)$  marks the amorphization of the vortex solid within the domains

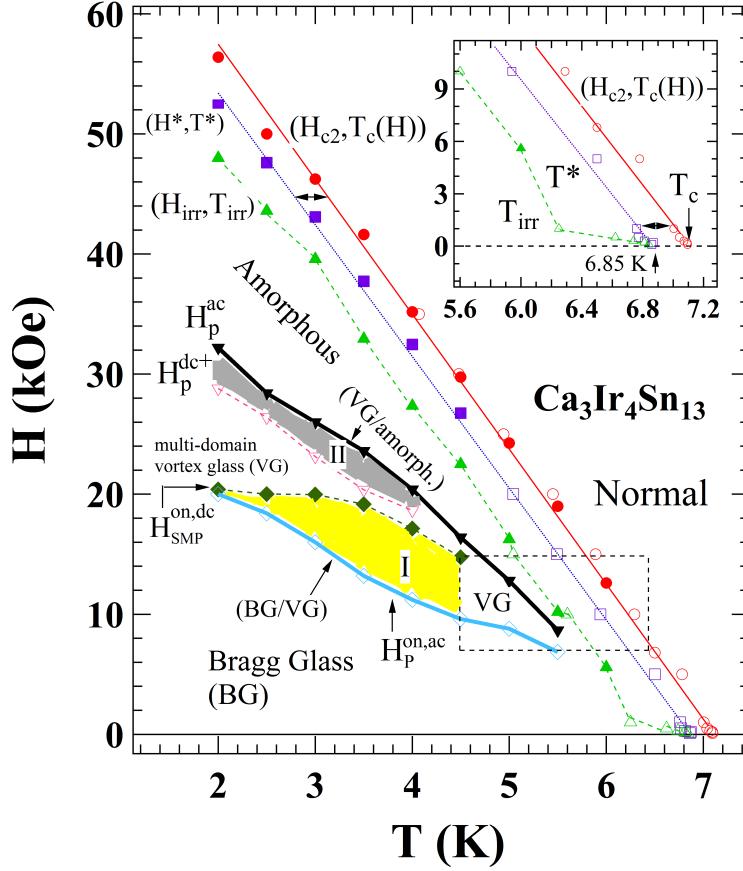


Figure 6: (Color online) Vortex phase diagram in the given  $\text{Ca}_3\text{Ir}_4\text{Sn}_{13}$  crystal, comprising phase boundaries obtained from both ac and dc magnetization data. Region-I enclosed between the onset of SMP ( $H_{SMP}^{\text{on},dc}(T)$  extracted from dc  $M$ - $H$  scans) and the onset of PE ( $H_p^{\text{on},ac}(T)$  obtained from ac  $\chi'(H)$ ) corresponds to the  $(H-T)$  phase space where an ac drive promotes disordering. Contrary to this, in the region-II bounded by the peak fields ( $H_p^{\text{ac}}(T)$  obtained from ac  $\chi'(H)$ ) of the PE and the SMP ( $H_p^{\text{dc}+}(T)$  extracted from dc  $M$ - $H$  scans) anomalies, an imposition of an ac drive shows an improvement in ordering. The characteristics field  $H^*(T)$  (as obtained in Fig. 5) lies between  $H_{irr}$  and  $H_{c2}$  as shown. Inset shows that  $H^*$  and  $H_{c2}$  remain well separated even in the close proximity of  $T_c$ .

in response to the collapse of its elasticity. In this region ( $T > 4.5$  K and  $6.8 \text{ kOe} < H < 15 \text{ kOe}$ ), the  $H_p^{\text{ac}}(T)$  line is in closer proximity of the irreversibility ( $H_{irr}, T_{irr}$ ) line. We recall that in a weakly-pinned conventional superconductors, where the PE phenomenon extends over a narrow  $(H, T)$  region and the irreversibility line lies in close proximity of the peak field/temperature of the PE, peak field of PE and/or the irreversibility line can be identified as the melting line. The vortex matter in between  $H_p^{\text{ac}}(T)$  and  $H_{irr}(T)$  is often termed to be pinned liquid. Therefore, in the boxed region ( $T > 4.5$  K and  $6.8 \text{ kOe} < H < 15 \text{ kOe}$ ), the  $H_{irr}(T)$  could be accepted as the melting line. In  $(H, T)$  domain, where the peak field/temperature of the PE is located far away from the irreversibility line (as in the interval  $T < 4.5$  K and  $H > 15 \text{ kOe}$ ), the vortex matter above the peak field of the SMP/PE perhaps comprises an admixture of pinned liquid and amorphous solid phases.

We now focus attention on to the reversible region bounded in between  $(H_{irr}, T_{irr})$  and  $(H_{c2}, T_c)$  lines in

the main panel of Fig. 6. It can be seen that the  $H_{c2}$  enhances in a linear way as temperature decreases below the superconducting transition temperature of 7.1 K. The irreversibility line also displays linear variation below  $T \sim 6.2$  K. The inset in Fig. 6 shows that above  $T = 6.2$  K, the irreversibility line has a long tail, which appears to terminate near  $T = 6.85$  K as  $H \rightarrow 0$ . In Fig. 6, we have also chosen to plot the  $(H^*, T^*)$  data points obtained from linear extrapolation of the reversible magnetization response, they lie in between the irreversibility and the  $H_{c2}(T)$  lines. It is instructive to note that  $H^*(T)$  runs parallel to the  $H_{c2}(T)$  line and it also meet the  $T = 0$  axis at  $T \sim 6.85$  K, distinct from the  $T_c$  value of 7.1 K. If one asserts that the reversible magnetization represents an equilibrium magnetization response and concerns with the mean field description of a type-II superconductor which predicts linear magnetization response, one may conclude that the superconducting-normal transition ought to terminate at  $H^*/T^*$ , rather than its extension up to a higher field ( $H_{c2}$ )/higher tem-

Table I: Superconducting parameters estimated for  $\text{Ca}_3\text{Ir}_4\text{Sn}_{13}$  using the GL theory at  $T = 2\text{ K}$ 

$\lambda$	$\xi$	$H_{c1}$	$H_{c2}$	$\kappa$	$G_i$	$j_c/j_0$ (at 15 kOe)
2712 Å	76 Å	80 Oe	56.4 kOe	$\sim 35$	$\sim 1.5 \times 10^{-8}$	$\sim 10^{-5}$

perature ( $T_c$ ) as apparent from the  $M(H)/M(T)$  plots (cf. Fig. 5). The deviation from the mean field description near the superconducting transition in the case of  $\text{Ca}_3\text{Ir}_4\text{Sn}_{13}$  deserves a more detailed understanding. The recent observation of ferromagnetic spin fluctuations in  $\text{Ca}_3\text{Ir}_4\text{Sn}_{13}$  [47] could be advanced as a rationale for these deviations, however, such a surmise may get discounted from the argument that the application of high fields ought to suppress the spin fluctuations, whereas in the present case, the separation between  $H^*(T)$  and  $H_{c2}(T)$  lines actually enhances at larger field values as apparent from Fig. 6.

## V. SUMMARY

To summarize, we have explored the vortex phase diagram in a weakly-pinned single crystal of a low  $T_c$  superconductor,  $\text{Ca}_3\text{Ir}_4\text{Sn}_{13}$ , which is attracting adequate attention in the recent literature for its novel physics. Table-1 contains various superconducting parameters evaluated (at  $T = 2\text{ K}$ ) for  $\text{Ca}_3\text{Ir}_4\text{Sn}_{13}$ , using the Ginzburg-Landau theory. The weak pinning nature of this compound is reflected by the ratio of depinning and depairing current densities ( $j_c/j_0$ )  $\sim 10^{-5}$ . The smallness of this ratio may be attributed to the presence of point defects and metallurgical source [57] of disorder in such compounds. The ac susceptibility ( $\chi'(H, T)$ ) measurements have revealed the occurrence of PE phenomenon in this compound. On the other hand, the results of dc magnetization measurements reflect features typically identified with the second magnetization peak anomaly. The phase boundaries constructed by both the ac as well as the dc data prompt us to identify the metastable regions in the vortex phase diagram of this compound. The region lying between the onset lines of the SMP ( $H_{SMP}^{on,dc}(T)$ ) in dc data and the PE like phenomenon ( $H_p^{on,ac}(T)$ ) in the ac data is taken as a superheated ordered vortex matter, which sees an enhancement in spatial disordering under the influence of an ac field. In contrast to this, the region lying between the peak field of the PE ( $H_p^{ac}$ ) and the SMP ( $H_p^{dc+}$ ) anomalies exhibits enhancement in the ordering due to the effect of an ac drive. Such an effect ceases at higher temperatures ( $T > 4.5\text{ K}$ ) because of the absence of the SMP fea-

ture there, only PE stands depicted at  $T > 4.5\text{ K}$  and for field values lying between 5 kOe and 15 kOe. The region of the  $H-T$  phase space over which the anomalous variation in  $j_c(H)$  predominates, is very broad and it bears resemblance with anomalous data in several other low  $T_c$  as well as high  $T_c$  superconductors, including the Cuprates. The broad (H,T) region comprises per se two transitions, a Bragg glass (BG) to vortex glass (VG) transition commencing at  $H_p^{on,ac}(T)$  (as in Fig. 6 for  $\text{Ca}_3\text{Ir}_4\text{Sn}_{13}$ ) and the amorphization of the vortex matter commencing at  $H_p^{dc+}(T)$  (as in Fig. 6). The  $H_p^{ac}(T)$  line for  $\text{Ca}_3\text{Ir}_4\text{Sn}_{13}$  in Fig. 6 can be taken to mark the spinodal line of the second transition. The gap between  $H_p^{dc+}$  and  $H_p^{ac}$  values progressively decreases as T approaches 4.5 K, and at 5 K, the said difference ceases to exist as the PE in the ac susceptibility subsumes the notion of SMP.

In the end, we may point out that the vortex phase diagram (Fig. 6) of  $\text{Ca}_3\text{Ir}_4\text{Sn}_{13}$  also raises an important issue regarding the source of diamagnetic response between  $H^*/T^*$  and  $H_{c2}/T_c$ . As per the G-L theory, the expected upper critical field/temperature should have been the ( $H^*, T^*$ ) line in Fig. 6, the experimental values of the same are slightly enhanced to ( $H_{c2}, T_c$ ) line. There is a significant separation between the two lines ( $(H^*, T^*)$  and  $(H_{c2}, T_c)$ ) even in an infinitesimally small field, as they intersect the temperature axis at  $T \sim 6.85\text{ K}$  and  $T_c$ , respectively. It is also pertinent to note that the G-L theory does not explicitly take into account the spatial ordering of the vortex matter. We have witnessed a reversible (amorphous) region (in the dc  $M(H)/M(T)$  response) that emerged from the disordered configuration (PE) of the vortex matter, wherein (i.e., above  $(H^*, T^*)$  line) the mean field description does not hold. A possible source for such an unusual observation could be the existence of surface superconductivity [58] above the  $H^*/T^*$  line and surviving up to the  $H_{c2}/T_c$  line in the  $H-T$  phase space. Efforts to explore this region of vortex phase diagram are currently in progress [59], with some significant success in sight.

## Acknowledgments

Santosh Kumar would like to thank the Council of Scientific and Industrial Research, India for grant of the Senior Research Fellowship.

## References

- 
- [1] G. Blatter, M. V. Feigel'man, V. B. Geshkenbein, A. I. Larkin, V. M. Vinokur, Rev. Mod. Phys. 66 (1994) 1125, and references therein.
  - [2] M. J. Higgins and S. Bhattacharya, Physica C 257 (1996) 232 and references therein.
  - [3] S. Bhattacharya, M. J. Higgins, Phys. Rev. Lett. 70



- (1993) 2617.
- [4] T. Giamarchi and P. Le Doussal, *Phys. Rev. Lett.* 72 (1994) 1530.
  - [5] T. Giamarchi and P. Le Doussal, *Phys. Rev. B* 52 (1995), 1242.
  - [6] T. Giamarchi, P. Le Doussal, *Phys. Rev. B* 55 (1997) 6577.
  - [7] S. S. Banerjee, S. Saha, N. G. Patil, S. Ramakrishnan, A. K. Grover, S. Bhattacharya, G. Ravikumar, P. K. Mishra, T. V. C. Rao, V. C. Sahni, C. V. Tomy, G. Balakrishnan, D. McK Paul, M. J. Higgins, *Physica C* 308 (1998) 25-32.
  - [8] S. S. Banerjee, A. K. Grover, M. J. Higgins, Gutam I. Menon, P. K. Mishra, D. Pal, S. Ramakrishnan, T. V. Chandrasekhar Rao, G. Ravikumar, V. C. Sahni, S. Sarkar, C. V. Tomy, *Physica C* 355 (2001) 39-50 and references therein.
  - [9] T. Nishizaki and N. Kobayashi, *Supercond. Sci Technol.* 13 (2000) 1.
  - [10] X. S. Ling and J. I. Budnick, in *Magnetic Susceptibility of Superconductors and Other Spin Systems*, edited by R. A. Hein, T. L. Francavilla and D. H. Leibenberg, Plenum, New York, 1991, pp. 377-388.
  - [11] G. D'Anna, W. Benoit, W. Sadowski and E. Walker, *Europhys. Lett.* 20 (1992) 167.
  - [12] H. Kupfer, Th. Wolf, C. Lessing, A. A. Zhukov, X. Lancan, R. Meier-Hirmer, W. Schauer and H. Wuhl, *Phys. Rev. B* 58 (1998) 2886 and references therein.
  - [13] S. Kokkaliaris, P. A. J. de Groot, S. N. Gordeev, A. A. Zhukov, R. Gagnon and L. Taillefer, *Phys. Rev. Lett.* 82 (1999) 5116.
  - [14] D. Pal, D. Dasgupta, B. K. Sarma, S. Bhattacharya, S. Ramakrishnan and A. K. Grover, *Phys. Rev. B* 62 (2000) 6699 and references therein.
  - [15] D. Pal, S. Ramakrishnan, A. K. Grover, D. Dasgupta and B. K. Sarma, *Phys. Rev. B* 63 (2001) 132505.
  - [16] S. Sarkar, D. Pal, P. L. Paulose, S. Ramakrishnan, A. K. Grover, C. V. Tomy, D. Dasgupta, B. K. Sarma, G. Balakrishnan and D. McK Paul, *Phys. Rev. B* 64 (2001) 144510.
  - [17] A. I. Larkin, Yu N. Ovchinnikov, *Sov. Phys. JETP* 38 (1974) 854.
  - [18] M. Daeumling, J. M. Seuntjens, D. D. Larbalestier, *Nature (London)* 346 (1990) 332.
  - [19] E. Zeldov, D. Majer, M. Konczykowski, V. B. Geshkenbein, V. M. Vinokur, H. Shtrikman, *Nature (London)* 375 (1995) 373.
  - [20] B. Khaykovich, E. Zeldov, D. Majer, T. W. Li, P. H. Kes and M. Konczykowski, *Phys. Rev. Lett.* 76 (1996) 2555.
  - [21] D. Giller, B. Kalisky, I. Shapiro, B. Ya Shapiro, A. Shaulov, Y. Yeshurun, *Physica C* 388-389 (2003) 731.
  - [22] Z. J. Huang, H. H. Fang, Y. Y. Xue, P. H. Hor, C. W. Chu, M. L. Norton and H. Y. Tang, *Physica C* 180 (1991) 331.
  - [23] S. N. Barilo, V. I. Gatal'skaya, S. V. Shiryayev, A. S. Sheshtac, L. A. Kurochkin, T. V. Smirnova, V. T. Koyava, N. S. Orlova and A. V. Pushkarev, *Physica C* 254 (1995) 181-188.
  - [24] W. Harneit, T. Klein, C. Escribano-Filippini, H. Rakoto, J. M. Broto, A. Sulpice, R. Buder, J. Marcus and W. Schmidbauer, *Physica C* 267 (1996) 270.
  - [25] P. L. Gammel, U. Yaron, A. P. Ramirez, D. J. Bishop, A. M. Chang, R. Ruel, L. N. Pfeiffer, E. Bucher, G. D'Anna, D. A. Huse, K. Mortensen, M. R. Eskildsen, and P. Kes, *Phys. Rev. Lett.* 80 (1998) 833.
  - [26] X. S. Ling, S. R. Park, B. A. McClain, S. M. Choi, D. C. Dender and J. W. Lynn, *Phys. Rev. Lett.* 86 (2001) 712.
  - [27] P. Das, C. V. Tomy, S. S. Banerjee, H. Takeya, S. Ramakrishnan and A. K. Grover, *Phys. Rev. B* 78 (2008) 214504.
  - [28] U. Yaron, P. L. Gammel, D. A. Huse, R. N. Kleiman, C. S. Oglesby, E. Bucher, B. Batlogg, D. J. Bishop, K. Mortensen, K. Clausen, C. A. Bolle and F. de la Cruz, *Phys. Rev. Lett.* 73 (1994) 2748.
  - [29] C. A. Bolle, F. de la Cruz, P. L. Gammel, J. V. Waszczak and D. J. Bishop, *Phys. Rev. Lett.* 71 (1993) 4039.
  - [30] A. M. Troyanovski, M. van Hecke, N. Saha, J. Aarts and P. H. Kes, *Phys. Rev. Lett.* 89 (2002) 147006.
  - [31] D. Pal, S. Ramakrishnan, A. K. Grover, M. J. Higgins and M. Chandran, *Physica C* 369 (2002) 200-208 and references therein.
  - [32] A. D. Thakur, S. S. Banerjee, M. J. Higgins, S. Ramakrishnan and A. K. Grover, *Phys. Rev. B* 72 (2005) 134524.
  - [33] A. D. Thakur, T. V. Chandrasekhar Rao, S. Uji, T. Terashima, M. J. Higgins, S. Ramakrishnan and A. K. Grover, *J. Phys. Soc Jpn* 75 (2006) 074718.
  - [34] D. Jaiswal-Nagar, A. D. Thakur, D. Pal, H. Takeya, S. Ramakrishnan and A. K. Grover, *Phys. Rev. B* 74 (2006) 184514.
  - [35] Pradip Das, C. V. Tomy, H. Takeya, S. Ramakrishnan and A. K. Grover *Physica C* 469 (2009) 151.
  - [36] C. V. Tomy, G. Balakrishnan and D. McK Paul, *Phys. Rev. B* 56 (1997) 8346.
  - [37] S. Sarkar, P. L. Paulose, S. Ramakrishnan, A. K. Grover, C. V. Tomy, G. Balakrishnan, D. McK Paul, *Physica C* 356 (2001) 181.
  - [38] S. Sarkar, D. Pal, S. S. Banerjee, S. Ramakrishnan, A. K. Grover, C. V. Tomy, G. Ravikumar, P. K. Mishra, D. McK Paul, S. Bhattacharya, *Phys. Rev. B* 61 (2000) 12394.
  - [39] M. Suresh Babu, A. Thamizhavel, S. Ramakrishnan, C. V. Tomy, A. K. Grover and D. Pal *Supercond. Sci. Technol.* 26 (2013) 125016.
  - [40] H. Sato, Y. Aoki, H. Sugawara and T. Fukuhara, *J. Phys. Soc. Jpn.* 64 (1995) 3175.
  - [41] C. V. Tomy, G. Balakrishnan and D. McK Paul, *Physica C* 280 (1997) 1.
  - [42] D. Pal, S. Ramakrishnan, A. K. Grover, D. Dasgupta and B. K. Sarma, *Supercond. Sci. Technol.* 15 (2002) 258.
  - [43] N. Avraham, B. Khaykovich, Y. Myasoedov, M. Rappaport, H. Shtrikman, D. E. Feldman, T. Tamegai, P. H. Kes, M. Li, M. Konczykowski, K. van der Beek, E. Zeldov *Nature* 411 (2001) 451.
  - [44] J. Kierfeld and V. Vinokur, *Phys. Rev. B* 69 (2004) 024501.
  - [45] P. Das, Ajay D. Thakur, Anil K. Yadav, C. V. Tomy, M. R. Lees, G. Balakrishnan, S. Ramakrishnan and A. K. Grover, *Phys. Rev. B* 84 (2011) 214526.
  - [46] G. P. Espinosa: *Mater. Res. Bull.* 15 (1980) 791.
  - [47] J. Yang, B. Chen, C. Michioka, K. Yoshimura, *J. Phys. Soc. Jpn.* 79 (2010) 113705.
  - [48] S. Y. Zhou, H. Zhang, X. C. Hong, B. Y. Pan, X. Qiu, W. N. Dong, X. L. Li and S. Y. Li, *Phys. Rev. B* 86 (2012) 064504.
  - [49] J. P. Remeika, G. P. Espinosa, A. S. Cooper, H. Barz, J. M. Rowell, D. B. McWhan, J. M. Vandenberg, D. E. Moncton, Z. Fisk, L. D. Wolf, H. C. Hamaker, M. B. Maple, G. Shirane and W. Thomlinson, *Solid State Commun.* 34 (1980) 923.

- [50] J. Ge, J. Gutierrez, J. Li, J. Yuan, H. B. Wang, K. Yamaura, E. Takayama-Muromachi and V. V. Moshchalkov, Phys. Rev. B 88 (2013) 144505.
- [51] E. Zeldov, A. I. Larkin, V. B. Geshkenbein, M. Konczykowski, D. Majer, B. Khaykovich, V. M. Vinokur and H. Shtrikman, Phys. Rev. Lett. 73 (1994) 1428.
- [52] Y. Paltiel, E. Zeldov, Y. N. Myasoedov, H. Shtrikman, S. Bhattacharya, M. J. Higgins, Z. L. Xiao, E. Y. Andrei, P. L. Gammel and D. J. Bishop, Nature (London) 403 (2000) 398.
- [53] C. P. Bean, Rev. Mod. Phys. 36 (1964) 31.
- [54] W. A. Fietz and W. W. Webb, Phys. Rev. 178 (1969) 657.
- [55] M. Tinkham, Introduction to Superconductivity, 2<sup>nd</sup> ed., McGraw-Hill International Edition 1996.
- [56] S. S. Banerjee, N. G. Patil, S. Ramakrishnan, A. K. Grover, S. Bhattacharya, G. Ravikumar, P. K. Mishra, T. V. Chandrasekhar Rao, V. C. Sahni, M. J. Higgins, Appl. Phys. Lett. 74 (1999) 126.
- [57] S. J. Levett, PhD thesis, University of Warwick, UK (2003).
- [58] D. Saint-James and P. G. de Gennes, Phys. Lett. 7 (1963) 306.
- [59] Santosh Kumar *et al.* unpublished.